JOURNAL OF AIRCRAFT
Vol. 45, No. 2, March–April 2008

Surface Integral Methods in Jet Aeroacoustics: Refraction Corrections

F. L. Pan*
International Truck and Engine Corporation, Fort Wayne, Indiana 46803-2926
A. Uzun†
Florida State University, Tallahassee, Florida 32306-4120
and
A. S. Lyrintzis‡
Purdue University, West Lafayette, Indiana 47906-2045

DOI: 10.2514/1.23513

One of the major challenges in computational jet aeroacoustics is the accurate modeling and prediction of acoustic fields to reduce and control the jet noise. Surface integral methods (e.g., the Kirchhoff method and Ffowcs Williams–Hawkings method) can be used in computational aeroacoustics to extend the near-field computational fluid dynamics results to far field. The surface integral methods can efficiently and accurately predict aerodynamically generated noise provided the control surface surrounds the entire source region. However, for jet noise prediction, shear mean flow exists outside the control surface that causes refraction. Mean flow refraction corrections for the surface integral methods have been done in the past using simple geometric acoustics. A more rigorous method based on Lilley's equation is investigated here due to its more realistic assumption of the acoustic propagation. Jet noise computational results based on large-eddy simulation for the near field of an isothermal jet at Reynolds number 400,000 are used for the evaluation of the solution on the Ffowcs Williams–Hawkings control surface. The proposed methodology for prediction of far-field sound pressure level shows that the acoustic field within the zone of silence is consistent with the measured data.

Nomenclature

Ai	=	Airy function
a	=	local sound speed normalized by its ambient value, $a \equiv \overline{a}/a_0$
$\mathcal{G}_\omega$	=	free-space Green's function in time domain
G_ω	=	fundamental solution of Fourier transformed wave equation defined by Eq. (17)
$\mathbf{G}_\omega$	=	fundamental solution of Fourier transformed wave equation defined by Eq. (18)
k_0	=	streamwise wave number, $k_0 = \omega/a_0$
$\mathcal{L}$	=	wave operator
M	=	Mach number or mean Mach number profile
n	=	critical azimuthal wave number
$\hat{n}_j$	=	outward directed unit normal vector
P_{ij}	=	compressive stress tensor with the constant $p_0\delta_{ij}$ subtracted
p	=	local pressure
Q	=	arbitrary function defined by Eq. (19)
q	=	arbitrary function defined by Eq. (19)
R	=	distance between observer and source point
Re_D	=	Reynolds number based on jet diameter
$\mathcal{R}_\omega$	=	arbitrary function defined by Eq. (19) or (20)
r	=	magnitude of radiation vector, $\lvert r_j \rvert$
r_δ	=	turning point defined by Eq. (19)
S	=	closed surface defined by $f(y, \tau)$
Sr	=	Strouhal number
t	=	time or observer reception time
U	=	mean velocity or mean velocity profile
u_i	=	Cartesian surface velocity components
$(\boldsymbol{x}, t)$	=	observer coordinates and time
Γ	=	acoustic source distribution
$\Delta\varphi$	=	difference in azimuthal angles of the observer and source point coordinates
δ_{ij}	=	Kronecker delta
ϑ	=	sound propagation angle
ϵ	=	arbitrary function defined by Eq. (19)
η	=	arbitrary function defined by Eq. (19)
θ	=	source emission angle
ξ	=	arbitrary function defined by Eq. (20)
Π	=	acoustic pressure fluctuation normalized by $\bar{\rho}\bar{a}^2$
ρ	=	fluid density
ζ	=	arbitrary function defined by Eq. (14)
τ	=	retarded or emission time, $t - R/a_0$
ϕ	=	acoustic variable
ω	=	cyclic frequency
$\langle\,\rangle$	=	root mean square evaluation

Subscripts

av	=	average parameter
c	=	corrected parameter
cr	=	critical angle parameter
J	=	quantity on jet centerline
m	=	measured parameter
n	=	inner product with $\hat{n}_j$
r	=	inner product with $\hat{r}_j$
ref	=	reference parameter
s	=	quantity evaluated at source position
ret	=	quantity evaluated at retarded time τ
0	=	ambient or freestream quantity

Presented as Paper 2873 at the 10th AIAA/CEAS Aeroacoustics Conference, Manchester, United Kingdom, May 2004; received 27 February 2006; accepted for publication 10 September 2007.

*Aerothermal Engineer.
†Postdoctoral Research Associate, School of Computational Science and Information Technology. Senior Member AIAA.
‡Professor, School of Aeronautics and Astronautics. Associate Fellow AIAA.

Superscripts

$'$	=	perturbation quantity, e.g., $\rho' = \rho - \rho_o$
$\dot{}$	=	source time derivative
$\bar{}$	=	mean flow quantity
$\widehat{}$	=	Fourier transformed quantity
$\hat{}$	=	unit vector

I. Introduction

COMPUTATIONAL aeroacoustics (CAA) is concerned with the prediction of the aerodynamic sound source and the propagation of the generated sound. The sound is generated by a nonlinear process, which is governed by the full, time-dependent, and compressible Navier–Stokes equations. Indeed, as the acoustic far field is linear and irrotational, one can consider two distinct processes, i.e., the nonlinear generation of sound and the linear propagation of sound. This implies that, instead of solving the full nonlinear flow equations out in the far field for sound propagation, one can extend the nonlinear near-field acoustic sources to the linear far-field sound through the traditional Lighthill's acoustic analogy [1] or surface integral methods, i.e., Kirchhoff's method [2], and Ffowcs Williams–Hawkings (FW-H) method [3,4]. The latter methods are more attractive as the volume integration is avoided. The surface integral methods assume that the sound propagation is governed by the simple wave equation, and can efficiently and accurately predict aerodynamically generated sound provided the control surface surrounds the entire nonlinear source region [5,6]. However, in jet noise prediction, the control surface cannot enclose the entire aerodynamic generated source region. Also, there is sheared mean flow downstream of the control surface. Thus, the linear wave equation is invalid when sound propagates through the region near the jet axis, downstream of the control surface.

In the past, researchers using surface integral methods to predict jet noise had ignored sound generated at and outside of the downstream end of the integration (control) surface [5]. These sources have a very small influence on the resulting sound, as shown by Uzun [7] using the MGB code [8] for typical grids used in large-eddy simulation (LES) of jet flows. The main effect is from the mean sheared flow outside the control surface. When acoustic waves propagate through the jet mean flow downstream of the control surface, they cross velocity-shear interfaces, which deflects the radiated sound away from the mean flow direction. This effect is called refraction [9]. For isothermal or hot jets, the effect of refraction gives rise to a "zone of silence," a region where a substantial reduction of sound occurs. Early investigations [9–11] found that the waves propagating in the zone of silence initially start as evanescent waves near the source. The presence of the zone of silence was also measured experimentally [12–14]. Surface integral methods are not able to predict the refraction outside the control surface and the resulting zone of silence. The mean flow refraction corrections to the surface integral method have been investigated using the simple geometric acoustics (GA) approximation [6,15], but no applications were given. This approximation is valid only for high frequencies. However, azimuthal variations between the sources in the sheared layer and the observers are not taken into account and hence the accuracy of this correction may be limited. It is worthwhile to attempt a more rigorous approach to achieve a more reliable prediction. A linearized homogeneous third-order convective wave equation, namely, Lilley's equation [16], has been solved asymptotically using the stationary phase method in the far field [9]. The high-frequency limit solution [17] of Lilley's equation is revisited and applied to refraction corrections of surface integral methods. The frequency range in which the approximation solution of Lilley's equation holds, is also studied.

The remainder of the paper revisits the surface integral formulations followed by a point source example to demonstrate the utility and efficiency of the refraction corrections schemes, i.e., GA method and Lilley's equation. This is achieved by coupling the surface integral methods with the refraction correction schemes. An application involving overall sound pressure level (OASPL) calculation based on an LES computation of an isothermal jet at $Re_D = 400,000$ is shown. Current calculation shows that the zone of silence is consistent with the measured data. An earlier version of this work was presented in [18].

II. Surface Integral Methodologies

A. Kirchhoff's Method

The Kirchhoff formula can be written as

$$4\pi\phi(\boldsymbol{x},t) = \int_S \frac{1}{R}\left[\frac{1}{a_\circ}\dot{\phi}\cos\theta - \frac{\partial\phi}{\partial n}\right]_{\text{ret}} \mathrm{d}S + \int_S \frac{[\phi]_{\text{ret}}}{R^2}\,\mathrm{d}S \quad (1)$$

where ϕ represents the acoustic variable, a_0 is the sound speed $\cos\theta = \hat{R}\cdot\hat{n}$, θ is the source emission angle, $\hat{n}$ is the outward directed unit normal vector of the closed control surface S, and R is the distance between the observer and the surface source. The surface integrals are over the control surface S and evaluated at retarded or emission time τ described by the following equation

$$\tau = t - \frac{R}{a_0} \quad (2)$$

where t is observer or reception time. The dependent variable ϕ is normally taken to be the disturbance pressure, but can be any quantity which satisfies the linear wave equation.

With the use of a Fourier transform, Eq. (1) can be expressed in the frequency domain (i.e., starting from Helmholtz equation) as

$$4\pi\widehat{\phi}(\boldsymbol{x},\omega) = \int_S e^{-i\omega R/a_\circ}\left[\frac{1}{R}\left(\frac{i\omega}{a_0}\cos\theta\widehat{\phi} - \frac{\partial\widehat{\phi}}{\partial n}\right) + \frac{\widehat{\phi}\cos\theta}{R^2}\right]\mathrm{d}S \quad (3)$$

where $\widehat{\phi}$ is the Fourier transform of ϕ, and ω is the cyclic frequency.

Equations (1) and (3) work well for aeroacoustic predictions when the control surface is placed in a region of the flowfield where the linear wave equation is valid. However, this might not be possible for some cases. Additional nonlinearities (i.e., quadrupoles) can be added outside the control Kirchhoff surface [19].

B. Porous Ffowcs Williams–Hawkings Method

The FW-H equation can be derived by introducing two new variables U_i and L_i (following Brentner and Farassat [20] and Di Francescantonio [21]),

$$U_i = \frac{\rho u_i}{\rho_0} \quad (4)$$

$$L_i = P_{ij}\hat{n}_j + \rho u_i u_n \quad (5)$$

where subscript 0 implies ambient conditions, superscript $'$ implies disturbances (e.g., $\rho = \rho' + \rho_0$), ρ is the density, u is the velocity, and P_{ij} is the compressive stress tensor with the constant $p_0\delta_{ij}$ subtracted. The integral form of the FW-H equation can be written as

$$p'(\boldsymbol{x},t) = p'_T(\boldsymbol{x},t) + p'_L(\boldsymbol{x},t) + p'_Q(\boldsymbol{x},t) \quad (6)$$

$$4\pi p'_T(\boldsymbol{x},t) = \int_S\left[\frac{\rho_0\dot{U}_n}{R}\right]_{\text{ret}}\mathrm{d}S \quad (7)$$

$$4\pi p'_L(\boldsymbol{x},t) = \frac{1}{a_0}\int_S\left[\frac{\dot{L}_r}{R}\right]_{\text{ret}}\mathrm{d}S + \int_S\left[\frac{L_r}{R^2}\right]_{\text{ret}}\mathrm{d}S \quad (8)$$

and the quadrupole noise pressure $p'_Q(\boldsymbol{x},t)$ can be determined by any method currently available. The subscript r or n indicates a dot product of the vector with the unit vector in the radiation direction $\hat{r}$ or the unit vector in the surface normal direction $\hat{n}_i$, respectively. It should be noted that the three pressure terms have a physical meaning for rigid surfaces: $p'_T(\boldsymbol{x},t)$ is known as thickness noise, $p'_L(\boldsymbol{x},t)$ is called loading noise, and $p'_Q(\boldsymbol{x},t)$ is called quadrupole noise. For a

porous surface, the terms lose their physical meaning, but the last term $p'_Q(\boldsymbol{x}, t)$ still denotes the quadrupoles outside surface S.

With the use of the Fourier transform, the FW-H formulation can be written in the frequency domain as

$$4\pi\widehat{p}'_T(\boldsymbol{x},\omega) = i\omega\int_S e^{-i\omega R/a_\circ}\frac{\rho_0\widehat{U}_n}{R}\,\mathrm{d}S \tag{9}$$

$$4\pi\widehat{p}'_L(\boldsymbol{x},\omega) = \frac{i\omega}{a_\circ}\int_S e^{-i\omega R/a_\circ}\frac{\widehat{L}_r}{R}\,\mathrm{d}S + \int_S\frac{\widehat{L}_r}{R^2}\,\mathrm{d}S \tag{10}$$

where $\widehat{p}'$, $\widehat{U}_n$, and $\widehat{L}_r$ are the Fourier transforms of p', U_n, and L_r, respectively, and ω is the cyclic frequency. Equations (6–10) provide a Kirchhoff-like formulation if the quadrupoles outside the control surface [$p'_Q(\boldsymbol{x}, t)$ term] are ignored.

III. Refraction Corrections

A. Geometric Acoustics

The application of simple geometric acoustics (GA) closed-form approximation used in this work is based on the thick cylindrical shear layer refraction correction [15,22]. This approximation is valid only when the acoustic wavelength is small compared with the shear layer thickness. First, we consider only mean flow effects on the sound radiation and model the wave propagation through a stratified medium, as described in Eq. (11),

$$\frac{a_0}{\cos\vartheta_0} = U + \frac{a_0}{\cos\theta} \tag{11}$$

where U is the steady velocity at the downstream end of the control surface, θ is the sound emission angle with respect to the jet axis, and ϑ_0 is the propagation angle in the stagnant, ambient air, as shown in Fig. 1. Equation (11) can be rearranged to show that the critical angle is defined by

$$\cos\theta_{\mathrm{cr}} = \frac{1}{1+M} \tag{12}$$

The critical angle θ_{cr} simply means that no sound can reach the observer and gives rise to the zone of silence.

This result is purely kinematic without taking the thick cylindrical shear layer refraction into account. The pressure correction factor parameter provides a more insightful refraction correction,

$$\left|\frac{P_c}{P_m}\right| = (1 - M\cos\vartheta_0)^2 \tag{13}$$

where P_c is the corrected pressure, and P_m is the measured pressure. Essentially, P_m is the far-field pressure fluctuation predicted from the Kirchhoff or FW-H method in the absence of the shear flow. An additional correction (not considered in [15]) is also used to account for the retarded source position, based on the following factor multiplication:

$$\frac{r_{\mathrm{ret}}}{r_c} = \frac{(1 - M\cos\vartheta_0)}{\sqrt{(1+M^2\zeta^2)}} \tag{14}$$

where $\zeta = \sqrt{(1 - M\cos\vartheta)^2 - \cos^2\vartheta}$. Therefore, Eqs. (13) and (14) can be used to add a mean flow refraction correction to a surface integral method (i.e., Kirchhoff or FW-H method).

One of the advantages of using the GA method is that it can be applied to a general source. This flexibility was arrived due to the separate corrections of the angle and amplitude. On the other hand, the azimuthal variation between the source and observer points has been ignored in the simple GA method. The azimuthal variations between the sources and observer points are important because the turbulence flow is highly exhibiting three-dimensional behavior in nature. We overcome this issue by introducing a more rigorous refraction method based on Lilley's equation [16], described next.

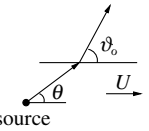

Fig. 1 Sound emission and propagation angle of a source due to refraction.

B. Lilley's Equation

Lilley's equation [16] is derived from the inhomogeneous wave equation. The equation describes explicitly the combined effects of sound convection and refraction by a unidirectional transversely sheared mean flow. Lilley's equation can be written as

$$\mathcal{L}\,\Pi = \Gamma \tag{15}$$

where Π denotes the acoustic pressure fluctuation normalized by $\bar{\rho}\bar{a}^2$, $\bar{\rho}$ is the mean flow density, $\bar{a}$ is the mean speed of sound, Γ represents the acoustic source distribution, and $\mathcal{L}$ is the wave operator originally derived by Pridmore-Brown [23].

$$\mathcal{L} = \frac{D}{Dt}\left(\frac{D^2}{Dt^2} - \nabla\bar{a}^2\nabla\right) + 2\bar{a}^2\nabla\bar{u}\nabla\frac{\partial}{\partial x} \tag{16}$$

where

$$\frac{D}{Dt} = \frac{\partial}{\partial t} + \bar{u}\frac{\partial}{\partial x}$$

is the convective derivative relative to mean flow, and $\bar{u}$ is the mean flow velocity.

In the past, many researchers [8,9,11] have tried to obtain the Green's function expression of Lilley's equation using a high-frequency, far-field asymptotic approximation. This approximation is valid only when the acoustics wavelength of the aerodynamic noise is much shorter than the characteristic length scale of the mean flow, and also the mean velocity profile is horizontal. At the end of the jet potential core, for example, the mean velocity profiles are significantly distorted, and the parallel mean flow assumption would fail.

Based on this assumption, three different closed forms of Green's function solution with locally parallel and axisymmetric mean flow were obtained. The first expression was developed by Goldstein [9], in which the source was placed on several wavelengths off the jet axis. At the same time, Balsa [11] developed an expression with the source located near the jet centerline axis. The third form was derived by Goldstein [24] with the implementation of ray-theory for parallel round jets. If a monopole source distribution is considered, the Green's function associated with the Fourier transformed solution of Lilley's wave equation $G_\omega(x|x_s)$ satisfies the following equation

$$\mathcal{L}[G_\omega(x|x_s)e^{-i\omega t}] = \frac{D}{Dt}[\bar{a}^2\delta(x - x_s)e^{-i\omega t}] \tag{17}$$

where ω is source frequency, x_s is source position, and δ is the Kronecker delta.

The fundamental solution of the Fourier transformed Lilley's equation, which is mathematically called the reduced Green's function, describes the effect of the surrounding mean flow on the radiated sound. Mean velocity gradients and temperature gradients are known to refract the acoustic energy within the mean shear layer. For simplicity, an isothermal jet condition is considered with no temperature gradients. Hence, the refraction is caused only by nonuniform mean flow within the shear layer, which varies radially at the outflow of the control surface. One can solve the reduced Green's function using a high-frequency asymptotic approximation.

As mentioned in [17], if the distance between the source and the jet centerline axis is sufficiently large (several factors of $1/k_0$, where k_0 is the streamwise wave number $k_0 = \omega/a_0$), then the critical azimuthal wave number n can be scaled to the order of k_0. This scaling was considered by Goldstein [9] and the resulting acoustic

field was referred to as the asymmetric, high-frequency approximation.

$$n = \mathcal{O}(k_0) \quad \text{as } k_0 \to \infty$$

On the other hand, as the source moves closer to the jet centerline axis, the scaling becomes

$$n = \mathcal{O}(1) \quad \text{as } k_0 \to \infty$$

Here, the critical wave number n scales like $1/r_J$, where r_J is the jet nozzle radius. This near-axis source problem was studied by Balsa [11] and the resulting acoustic field was referred to as the quasi-symmetric, high-frequency approximation.

Assuming both k_0 and $R \to \infty$, the following Eq. (18) gives the ratio of the reduced Green's function to the free-space Green's function, which was implemented in the refraction corrections codes developed in this research.

$$\frac{\mathbf{G}_\omega(x|x_s)}{\mathcal{G}_\omega(X|X_S)} \sim \frac{\mathcal{R}_\omega(X|X_S)}{a(r_s)[1 - M(r_s)\cos\theta]} \tag{18}$$

Based on the asymmetric and quasi-symmetric behaviors of the acoustic field, two distinct $\mathcal{R}_\omega(x|x_s)$ functions from Eq. (18) are derived in separate approaches and are used to describe the acoustic field accordingly. The asymmetric, high-frequency solutions are used for off-axis source locations, whereas the quasi-symmetric solutions are applied to near-axis locations.

For the asymmetric, far-field approximation, $\mathcal{R}_\omega(x|x_s)$ is defined by the following equation:

$$\mathcal{R}_\omega(x|x_s) \sim \sum_{n=-\infty}^{n=\infty} \left[\frac{2}{k_0}\frac{\sqrt{-\eta_n(r_s)}}{r_s Q_n(r_s)}\right]^{\frac{1}{2}} Ai[\eta_n(r_s)]\epsilon \tag{19}$$

where

$$\epsilon = e^{in\Delta\varphi + ik_0[\zeta_n(r) - R\sin^2\theta]} \qquad Q_n(r) = \sqrt{q^2(r) - \left(\frac{nk_0}{r}\right)^2}$$

$$q(r) = \sqrt{\left[\frac{1 - M(r)\cos\theta}{a(r)}\right]^2 - \cos^2\theta}$$

$$\eta_n(r) = -\left[\frac{3}{2}k_0\zeta_n(r)\right]^{\frac{2}{3}} \qquad \zeta_n(r) = \int_{r_\delta}^{r} Q_n(r)\,\mathrm{d}r, \qquad Q_n^2(r_\delta) = 0$$

where $a \equiv \bar{a}/a_0$ is the local sound speed normalized by its ambient value, $M = U/a_0$ is the Mach number based on the ambient speed of sound, $\Delta\varphi$ is the azimuthal difference between observer and source point, r_s is the source location, and Ai is the Airy function. Note that the cube root in the definition of η_n in Eq. (19) is taken such that $\eta_n < 0$ for $r > r_\delta$ and $\eta_n > 0$ for $r < r_\delta$.

For the quasi-symmetric, far-field approximation, $\mathcal{R}_\omega(x|x_s)$ is defined by the following equation:

$$\mathcal{R}_\omega(x|x_s) \sim e^{ik_0[\xi(r) - R\sin^2\theta - \xi(r_s)\cos\Delta\varphi]} \tag{20}$$

where

$$\xi(r) = \int_0^r q(r)\,\mathrm{d}r$$

Comparisons done in [18] for $|\mathbf{G}_\omega/\mathcal{G}_\omega|$ at various azimuthal-angle parameters $\Delta\varphi$ of both asymmetric and quasi-symmetric approximations using the case suggested in [17] show results identical to [17]. With different azimuthal-angle parameters $\Delta\varphi$, $|\mathbf{G}_\omega/\mathcal{G}_\omega|$ varies . This implies that simply ignoring the azimuthal variations between the source and the observer points may result in inaccurate predictions.

The first assumption in Eq. (19), i.e., $k_0 \to \infty$ needs to be well defined and the lowest wave number k_0 value should be correctly determined. An analysis was done for this evaluation in [17]. The same results are obtained here, which show the asymptotic high-frequency approximation for solutions of Lilley's equation remains accurate with Strouhal number as small as one-half. Below this Strouhal number limit, asymptotic approximation does not apply and the refraction correction must be done by an alternative way, which we choose to be the simple GA method.

Essentially, the asymmetric solution is implemented for all source elements except for a near-axis source, where the asymmetric solution breaks down and a quasi-symmetric solution is used. It should be noted that r_δ defined in Eq. (19) does not appear in Eq. (20). The solution r_δ for which the nonlinear equation Q_n is zero, and is called turning point and is determined by solving the equation numerically. Because of its dependency on velocity magnitude, which varies along the radial direction, the use of asymmetric approximation turns out more computationally expensive compared with the quasi-symmetric approximation.

IV. Validation Case: Point Source

A simple monopole is used to demonstrate the application of refraction corrections in jet noise prediction. This test case is not representative of jet noise, but shows the nature of the corrections. It is used because of its simplicity. Equation (3) is used for the Kirchhoff method, Eqs. (9) and (10) for the FW-H method, Eqs. (13) and (14) for the GA corrections, and Eqs. (18–20) for Lilley's equation method. Brent's method [25] is used for the numerical evaluation of the turning point r_δ in Eq. (19). The frequency domain version of the Ffowcs Williams–Hawkings integral was implemented to account for the acoustic far-field propagation of the noise source. A cylindrical control surface ($L_k = 40$, $r_k = 5$), as shown in Fig. 2, was considered in this demonstration. The point source is placed at the middle of the surface and the surface pressure is defined as

$$\widehat{p}(x_s, \omega) = \frac{1}{r_s} e^{-i\omega\frac{r_s}{a_0}} \tag{21}$$

The acoustics wave number k_0 of 1.0 is considered. We are using 20 points per wavelength. The distance between the midpoint of the cylinder's axis and the observer is taken to be $60r_J$, where r_J is 1. The result with no refraction correction is shown in Fig. 3. A normalized amplitude of one is expected with no mean flow outside the FW-H surface.

Assume there is a nonuniform shear flow at the right base of the cylinder control surface with the velocity profile (typical of jet flow) described by

$$M(r) = M_J e^{Ar^2} \tag{22}$$

where r is the radial distance, $M_J = 0.5$, and $A = -0.21$. The velocity variation impacts the far-field pressure contributed by those point sources acting at radial location. At surface radius of 5, the corresponding Mach number is 0.002, and the centerline Mach number is 0.5. Because velocity becomes negligible near the radial distance of 5, the refraction correction is applied only for $r < 5$.

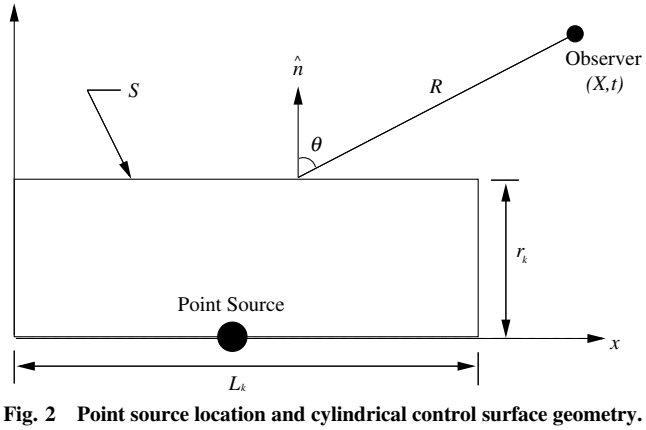

Fig. 2 Point source location and cylindrical control surface geometry.

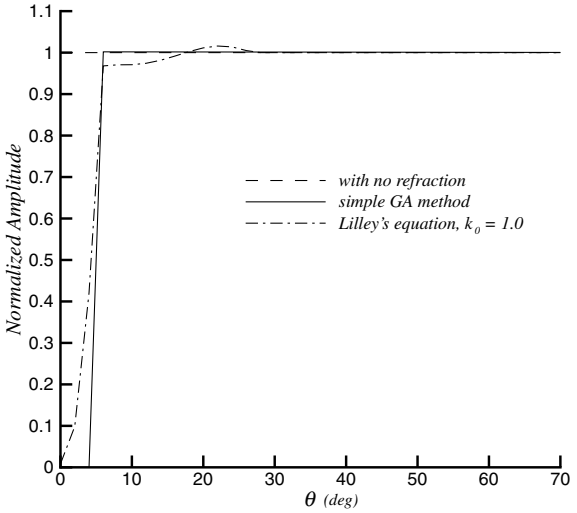

Fig. 3 Refraction effects.

As shown in Fig. 3, the normalized pressure amplitude shows an abrupt decrease within the shallow angles region for the GA case. Lilley's equation results in a relatively smooth amplitude decrease in the region. Similar results were obtained from the Kirchhoff method, and hence only the FW-H results are shown here.

V. Jet Noise Prediction Using Large-Eddy Simulation

The surface integral methods can extend the near-field computational fluid dynamics flow data to far-field acoustic properties, e.g., acoustic pressure. The near-field input for the surface integral methods is obtained from a large-eddy simulation calculation [7,26].

In this study, the LES calculation is performed for a turbulent isothermal round jet at a Mach number of 0.9 and Reynolds number of 400,000. The LES calculation employs an implicit sixth-order tridiagonal spatial filter [27] as the implicit subgrid-scale model. The jet centerline temperature was chosen to be the same as the ambient temperature T_0 and set to 286 K. A fully curvilinear grid consisting of approximately 16 million grid points was used in the simulation. The grid has 390 points along the streamwise x direction and 200 points along both the y and z directions. The physical portion of the domain in this simulation is extended to 35 jet radii in the streamwise direction and 30 jet radii in the transverse directions. The coarsest resolution in this simulation is estimated to be about 400 times the local Kolmogorov length scale.

The boundaries of the computational domain are treated using Tam and Dong's three-dimensional radiation and outflow boundary conditions [28]. A sponge zone [29] near the downstream surface is used in which grid stretching and artificial damping are applied to suppress the unwanted reflections from the outflow boundary. Because the actual nozzle geometry is not included in the present calculations, randomized perturbations in the form of a vortex ring are added to the jet velocity profile at a short distance downstream of the inflow boundary to excite the three-dimensional instabilities in the jet and cause the potential core of the jet to break up at a reasonable distance downstream of the inflow boundary. The inflow forcing used here was proposed by Bogey and Bailly [30]. There are about 14 grid points in the initial jet shear layer. The standard fourth-order explicit Runge–Kutta scheme is used for time advancement.

A Ffowcs William–Hawkings control surface was placed around the jet, as illustrated in Fig. 4. The control surface starts one jet radius downstream of the inflow boundary and extends to 31 jet radii along the streamwise direction. Hence, the total streamwise length of the control surface is $30r_J$. The control surface is initially at a distance of 3.9 jet radii from the jet centerline, and opens up with downstream distance. The LES flowfield data are gathered on the control surface in the time domain at every five times steps over a period of 25,000

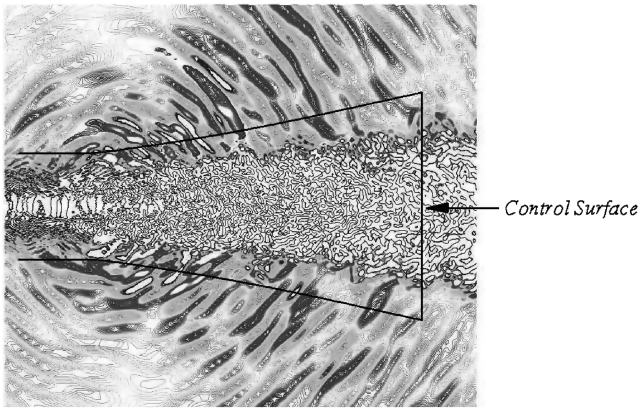

Fig. 4 Schematic of the control surface surrounding the jet flow.

time steps during the LES run. The initial transients exited the domain over the first 10,000 time steps. The total acoustic sampling period corresponds to a time scale in which an ambient sound wave travels about 14 times the domain length in the streamwise direction. Assuming at least six points per wavelength are needed to accurately resolve an acoustic wave, it is found that the maximum frequency resolved with the grid spacing around the control surface corresponds to a Strouhal number of approximately 3.0. This is the grid cutoff frequency used in computation domain. Based on the data sampling rate, the number of temporal points per period in this maximum frequency is eight.

To investigate results of the refraction corrections, a frequency domain of the FW-H method is developed and has LES data as an input at outflow surface. A 4608-point fast Fourier transform (FFT) analysis is performed to obtain the variables required in FW-H calculation, which are $\widehat{p}'$, $\widehat{U}_n$, and $\widehat{L}_r$ at each frequency. These terms are calculated in the retarded time algorithm using Eq. (2), which can be solved by performing a simple linear interpolation.

It should be noted that the refraction corrections evaluated on the downstream control surface are employing the frequency domain FW-H equation. These results are added to the time domain FW-H results for an open surface [26]. Thus, an inverse FFT is needed to recover the signal for the downstream refraction surface in the time domain.

Numerical results of far-field overall sound pressure level (OASPL) are calculated using Eq. (23) along an arc of radius $60r_J$ from the jet nozzle.

$$\text{OASPL} = 20\log_{10}\left(\frac{E}{P_{\text{ref}}}\right) \tag{23}$$

where P_{ref} is the nondimensional reference pressure calculated from the ambient temperature $T_0 = 286$ K, ambient pressure $p_0 = 1.01$ kPa, $M = 0.9$ at jet centerline nozzle exit, and dimensional reference pressure, 2×10^{-5} Pa. E is defined as $\langle \int P_{\text{av}}(f)\,\mathrm{d}f \rangle$, where P_{av} is calculated from the average acoustic pressure signals over the equally spaced 36 azimuthal points on a full circle at a given θ location on far-field arc of radius $60r_J$ from the jet nozzle. The center of the arc is chosen as the jet nozzle exit and the angle θ is measured from the jet axis as illustrated in Fig. 5.

One should remove the low frequencies resulting from the outflow boundary which may not be damped out effectively by the sponge zone. In our jet case, this frequency with the corresponding Strouhal number of 0.05 was found. Hence, the OASPL spectra integration only includes the resolved frequencies range of $0.05 \leq Sr \leq 3.0$.

The computations of surface integral method were performed on an IBM Power 3 machine at Purdue University. Advanced features offered by FORTRAN 90 such as dynamics memory allocation are implemented in the code to enable the computations. The codes are run in parallel using message passing interface (MPI) implementation. The outflow surface comprises of a total of 135×135 patches. The wall time required for computing acoustic signals at each arc location (with 36 azimuthal locations) from the outflow FW-H

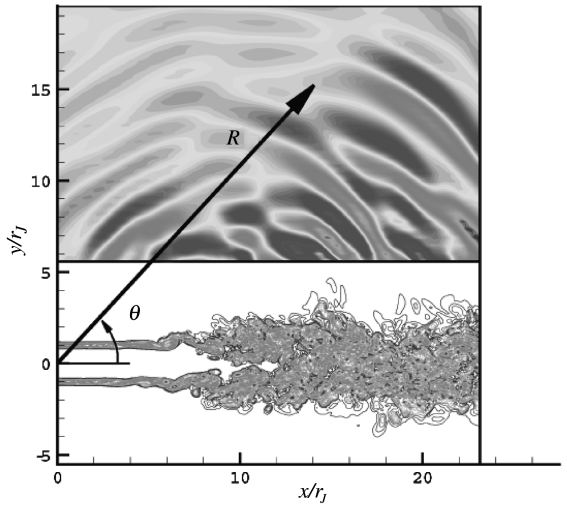

Fig. 5 Schematic showing the center of the arc and how the angle θ is measured from the jet axis.

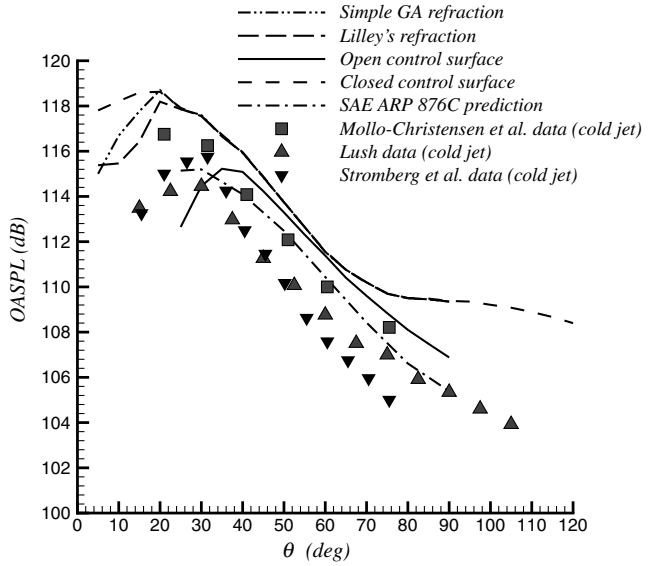

Fig. 6 Overall sound pressure levels at $60r_J$ from the nozzle exit.

surface is around 5.8 h using eight 375 MHz processors. The solutions of the rest of the FW-H surfaces are added to the solutions of the outflow surface that includes the refraction corrections. In Fig. 6, the solid line represents the OASPL result with no refraction correction at the observer location along a far-field arc of $x = 60r_J$. Table 1 summarizes the Mach numbers and Reynolds numbers of the experiments and the Aerospace Recommended Practice (ARP) database [33] that we are using for comparison. It should be noted that the experimental jets were cold jets, whereas our jet is an isothermal jet. However, as indicated in the ARP database, the effect of the temperature for this case is very small, i.e., about 0.3 dB.

From the OASPL plot for an open surface, it is shown that the prediction from the ARP database for a cold jet at Re_D of 400,000 is

Table 1 Some jet noise experiments with Mach numbers similar to that of our LES

M	Re_D	Reference
0.9	540,000	Mollo-Christensen et al. [31]
0.88	500,000	Lush [13]
0.9	3600	Stromberg et al. [32]
0.9	400,000	SAE ARP 876C [33]
0.9	400,000	our three-dimensional LES [7]

slightly lower (about 1 dB) than the LES calculations for high angles, i.e., $\theta \geq 40$ deg. This overprediction is typical of LES calculations (e.g., Bodony and Lele [34]) and could be possibly attributed to the noisy forcing. Also, the OASPL are comparable to the experimental values at these angles. However, at shallow angles, i.e., $\theta \leq 40$ deg, the OASPL from the LES drops significantly due to the omission of the signal from the downstream surface. For the closed control surface, the OASPL is generally higher than that of the open control surface. The results increase significantly for lower angles. However, there is a significant overprediction at angles $\theta \leq 20$ deg, as refraction effects outside the control surface are not included. For higher angles, i.e., $\theta \geq 70$ deg, there is also an overprediction due to an spurious line of dipoles on the downstream surface area, as the quadrupoles move downstream and exit the control surface [26].

The implementation of the refraction correction begins with generating a parallel shear mean flow. To reduce the required computational time for Lilley's equation, the mean flow velocity profile is modeled with the following equation

$$M(r) = M_J e^{Ar^2} + B \tag{24}$$

where $M_J = 0.46$, and A, B are constants, i.e., -0.14 and 0.0044, respectively. This is a curve-fit of the actual velocity from the LES code.

This profile is used for both the simple GA method and Lilley's equation calculations. This sheared mean flow has an influence on the signals emitted from the surface elements on the downstream outflow FW-H surface. Refraction corrections are performed on the surface elements inside the sheared flow, i.e., on the downstream surface. The variation of the velocities across the radial direction of the shear layer is taken into account at each surface element location. The refraction corrections schemes result in the damping of the far-field signal contributed by the surface element. Within the high-frequency region of $0.50 \leq Sr \leq 3.0$, these refraction corrections are performed at each frequency and on each surface element.

As shown in Fig. 6, the OASPL with refraction corrections starts to decrease as θ goes below 20 deg. This gives a zone of silence as expected from the experimental results. The slight decrease of the results with no refraction corrections is due to the existence of refraction inside the FW-H control surface. With the refraction corrections outside the control surface using the GA method, the results show a decrease on the OASPL, making it closer to the experiments. The results from the Lilley's equation method exhibit a smoother decrease on the OASPL inside the zone of silence, which is consistent with the results for a monopole source, shown in Fig. 3.

With the application of Lilley's equation, the computational wall time required increases to about 180 h for each arc location inside the zone of silence using eight 375 MHz processors run in parallel. The maximum time ratio for Lilley's equation method to GA method is 60. This significant increase in computational time is expected when solving Lilley's equation, because the mean flow velocity dependent turning point r_δ in Eq. (19) needs to be evaluated numerically.

VI. Conclusions

In the past, the surface integral methods have proven to be an efficient and accurate tool for the prediction of jet noise and other aeroacoustic phenomena. However, they fail to predict the zone of silence accurately. We have developed refraction corrections and used them with the surface integral methods, i.e., Kirchhoff and porous Ffowcs Williams–Hawkings methods. The refraction corrections are based on simple geometric acoustics and Lilley's equation high-frequency, far-field asymptotic solutions. The methods were applied to the noise calculation of an isothermal jet of Reynolds number 400,000. The solution on the FW-H control surface was provided using LES. The preceding refraction corrections were applied on the downstream control surface to account for the mean shear flow outside the control surface. Both refraction corrections improve the OASPL results dramatically at shallow angles near the axis.

Comparisons between the two methods were also made and it was shown that the simple GA method is much simpler and requires less computational time compared with Lilley's equation. On the other hand, the high-frequency asymptotic solutions for Lilley's equation has the potential of being more realistic, allowing azimuthal variations between source and observer. The use of the simple GA method and Lilley's equation have shown a successful prediction of the zone of silence by applying inexpensive extensions of the traditional surface integral methods, although a faster solution for Lilley's equation should be sought.

Acknowledgments

The simulations were carried out on Purdue University's 320 processor IBM-SP3 supercomputer. A. S. Lyrintzis acknowledges support by the Indiana 21st Century Research and Technology Fund, and the Aeroacoustics Research Consortium, a government and industry consortium managed by the Ohio Aerospace Institute. A. S. Lyrintzis would also like to thank Abbas Khavaran from NASA Glenn Research Center for suggesting the Lilley's equation method for refraction corrections. F. L. Pan is grateful to Gregory Blaisdell and Phoi-Tak Lew for providing useful suggestions and discussions.

References

[1] Lighthill, M. J., "On Sound Generated Aerodynamically, 1: General Theory," *Proceedings of the Royal Society of London, Series A: Mathematical and Physical Sciences*, Vol. 211, No. 1107, 1952, pp. 564–587.

[2] Kirchhoff, G. R., "Zur Theorie der Lichtstrahlen," *Annalen der Physik und Chemie*, Vol. 254, No. 4, 1883, pp. 663–695. doi:10.1002/andp.18832540409

[3] Ffowcs Williams, J. E., and Hawkings, D. L., "Sound Generation by Turbulence and Surfaces in Arbitrary Motion," *Proceedings of the Royal Society of London, Series A: Mathematical and Physical Sciences*, Vol. 264, No. 1151, 1969, pp. 321–342. doi:10.1098/rsta.1969.0031

[4] Crighton, D. G., Dowling, A. P., Ffowcs Williams, J. E., Heckl, M., and Leppington, F. G., *Modern Methods in Analytical Acoustics: Lecture Notes*, Springer–Verlag, London, 1992.

[5] Lyrintzis, A. S., "Surface Integral Methods in Computational Aeroacoustics: From the (CFD) Near-Field to the (Acoustic) Far-Field," *International Journal of Aeroacoustics* Vol. 2, No. 2, 2003, pp. 95–128. doi:10.1260/147547203322775498

[6] Lyrintzis, A. S., and Uzun, A., "Integral Techniques for Jet Aeroacoustics Calculations," *7th AIAA/CEAS Aeroacoustics Conference*, AIAA Paper 2001-2253, May 2001.

[7] Uzun, A., "3-D Large Eddy Simulation for Jet Aeroacoustics," Ph.D. Dissertation, School of Aeronautics and Astronautics, Purdue Univ., West Lafayette, IN, Dec. 2003.

[8] Mani, R., Gliebe, P. R., and Balsa, T. F., "High Velocity Jet Noise Source Location and Reduction," FAA RD-76-79-II, 1978.

[9] Goldstein, M. E., *Aeroacoustics*, McGraw–Hill, New York, 1976, Chap. 6.

[10] Tester, B. J., and Morfey, C. L., "Developments in Jet Noise Modelling: Theoretical Predictions and Comparisons with Measured Data," *Journal of Sound and Vibration*, Vol. 46, No. 1, May 1976, pp. 79–103. doi:10.1016/0022-460X(76)90819-1

[11] Balsa, T. F., "Far-Field of High Frequency Convected Singularities in Sheared Flows, with an Application to Jet Noise Prediction," *Journal of Fluid Mechanics*, Vol. 74, March 1976, pp. 193–208. doi:10.1017/S0022112076001766

[12] Atvars, J., Schubert, L. K., and Ribner, H. S., "Refraction of Sound from a Point Source Placed in an Air Jet," *Journal of the Acoustical Society of America*, Vol. 37, No. 1, Jan. 1965, pp. 168–170. doi:10.1121/1.1909297

[13] Lush, P. A., "Measurements of Subsonic Jet Noise and Comparison with Theory," *Journal of Fluid Mechanics*, Vol. 46, No. 3, 1971, pp. 477–500. doi:10.1017/S002211207100065X

[14] Tanna, H. K., "An Experimental Study of Jet Noise, Part 1: Turbulent Mixing Noise," *Journal of Sound and Vibration*, Vol. 50, No. 3, Feb. 1977, pp. 405–428. doi:10.1016/0022-460X(77)90493-X

[15] Pilon, A. R., and Lyrintzis, A. S., "Mean Flow Refraction Corrections for the Kirchhoff Method," *Journal of Aircraft*, Vol. 35, No. 4, July–Aug. 1998, pp. 661–664.

[16] Lilley, G. M., "On the Noise from Jet," AGARD CP 131, 1974, pp. 1–12.

[17] Wundrow, D. W., and Khavaran, A., "On the Applicability of High-Frequency Approximations to Lilley's Equation," NASA CR 2003-212089, 2003.

[18] Pan, F. L., Uzun, A., and Lyrintzis, A. S., "Refraction Corrections for Surface Integral Methods in Jet Aeroacoustics," AIAA Paper 2004-2873, 2004.

[19] Pilon, A. R., and Lyrintzis, A. S., "Development of an Improved Kirchhoff Method for Jet Aeroacoustics," *AIAA Journal*, Vol. 36, No. 5, May 1998, pp. 783–790.

[20] Brentner, K. S., and Farassat, F., "An Analytical Comparison of the Acoustic Analogy and Kirchhoff Formulations for Moving Surfaces," *AIAA Journal*, Vol. 36, No. 8, Aug. 1998, pp. 1379–1386.

[21] Di Francescantonio, P., "A New Boundary Integral Formulation for the Prediction of Sound Radiation," *Journal of Sound and Vibration*, Vol. 202, No. 4, 1997, pp. 491–509. doi:10.1006/jsvi.1996.0843

[22] Amiet, R. K., "Refraction of Sound by a Shear Layer," *Journal of Sound and Vibration*, Vol. 58, No. 4, 1978, pp. 467–482. doi:10.1016/0022-460X(78)90353-X

[23] Pridmore-Brown, D. C., "Sound Propagation in a Fluid Flowing Through an Attenuating Duct," *Journal of Fluid Mechanics*, Vol. 4, No. 4, Aug. 1958, pp. 393–406. doi:10.1017/S0022112058000537

[24] Goldstein, M. E., "High Frequency Sound Emission from Moving Point Multipole Sources Embedded in Arbitrary Transversely Shear Mean Flows," *Journal of Sound and Vibration*, Vol. 80, No. 4, Feb. 1982, pp. 499–522. doi:10.1016/0022-460X(82)90495-3

[25] Brent, R. P., *Algorithms for Minimization Without Derivatives*, Prentice–Hall, Englewood Cliffs, NJ, Chaps. 3–4, 1972

[26] Uzun, A., Lyrintzis, A. S., and Blaisdell, G. A., "Coupling of Integral Acoustics Methods with LES for Jet Noise Prediction," *International Journal of Aeroacoustics*, Vol. 3, No. 4, Dec. 2004, pp. 297–346. doi:10.1260/1475472043499290

[27] Visbal, M. R., and Gaitonde, D. V., "Very High-order Spatially Implicit Schemes for Computational Acoustics on Curvilinear Meshes," *Journal of Computational Acoustics*, Vol. 9, No. 4, 2001, pp. 1259–1286.

[28] Bogey, C., and Bailly, C., "Three-dimensional Non-Reflective Boundary Conditions for Acoustic Simulations: Far Field Formulation and Validation Test Cases," *Acta Acustica*, Vol. 88, No. 4, 2002, pp. 463–471.

[29] Colonius, T., Lele, S. K., and Moin, P., "Boundary Conditions for Direct Computation of Aerodynamic Sound Generation," *AIAA Journal*, Vol. 31, No. 9, 1993, pp. 1574–1582.

[30] Bogey, C., and Bailly, C., "Effects of Inflow Conditions and Forcing on a Mach 0.9 Jet and its Radiated Noise," *AIAA Journal*, Vol. 43, No. 5, 2005, pp. 1000–1007.

[31] Mollo-Christensen, E., Kolpin, M. A., and Martucelli, J. R., "Experiments on Jet Flows and Jet Noise Far-field Spectra and Directivity Patterns," *Journal of Fluid Mechanics*, Vol. 18, No. 2, Feb. 1964, pp. 285–301. doi:10.1017/S0022112064000209

[32] Stromberg, J. L., McLaughlin, D. K., and Troutt, T. R., "Flow Field and Acoustic Properties of a Mach Number 0.9 Jet at a Low Reynolds Number," *Journal of Sound and Vibration*, Vol. 72, No. 2, 1980, pp. 159–176. doi:10.1016/0022-460X(80)90650-1

[33] Society of Automotive Engineers, Gas Turbine Jet Exhaust Noise Prediction: ARP 876C, Society of Automotive Engineers, Warrendale, PA, Nov. 1985.

[34] Bodony, D., and Lele, S., "Review of the Current Status of Jet Noise Predictions Using Large-Eddy Simulations," *44th AIAA Aerospace Science Meeting and Exhibit*, AIAA Paper 2006-0468, Jan. 2006.